High-Pressure Far- and Mid-Infrared Study of 1,3,5-Triamino-2,4,6-trinitrobenzene

Michael Pravica,*,† Brian Yulga,† Sergey Tkachev,† and Zhenxian Liu‡

High Pressure Science and Engineering Center and Department of Physics, University of Nevada Las Vegas, Las Vegas, Nevada 89154-4002 and Geophysical Laboratory, Carnegie Institution of Washington, 5251 Broad Branch Road NW, Washington, D.C. 20015-1305

Received: December 31, 2008; Revised Manuscript Received: June 11, 2009

Synchrotron infrared measurements of 1,3,5-triamino-2,4,6-trinitrobenzene (TATB) have been performed in the far-IR and mid-IR spectral regions up to ~30 and ~40 GPa, respectively. For the far-IR experiment, no pressurizing medium was used, whereas KBr was utilized as a pressurizing medium for the mid-IR experiment. For both experiments, pressure was cycled and IR spectra were recorded at various pressures to ascertain sample survival. In the high frequency region (~3000 cm^{-1}) of the mid-IR spectra, the peak frequencies of the NH_2 symmetric and antisymmetric vibrational modes steadily decrease with increasing pressure, indicating strengthening of intermolecular hydrogen bonding with pressure. In both experiments, no apparent phase transition was observed to the highest pressures studied.

Introduction

"Insensitive" high explosives (IHEs) are a class of secondary explosives that are preferred to conventional high explosives (CHEs) and primary, sensitive explosives in situations that require safety from accidental detonation and better control.[1] Understanding precisely what makes insensitive explosives so relatively stable (as compared with CHEs and primary explosives) will aid in further development of munitions that will have a combination of high stability to mechanical, thermal, radiation, and electrical stimuli, retain the performance of CHEs, and perhaps allow the creation of energetic materials that can be sensitized or desensitized at will. To achieve this very challenging yet tantalizing level of control, the mechanism of detonation (which remains elusive) must be understood at the quantum/molecular level wherein the molecular alterations enabling transfer of mechanical energy in a shockwave to break bonds are poorly understood.[1] Under detonation conditions, a shockwave propagates through the material at supersonic speeds.[2] The high-temperature and high-pressure conditions behind the shockwave create the conditions that somehow transfer energy to the explosive releasing energy that further sustains the shockwave. There are a number of theories[3−5] that postulate the mechanism surrounding the transfer of energy but have not been verified. Experiments that aim to understand how the explosive molecules deform and ultimately behave under the real-time conditions of a shockwave are very challenging. Therefore, static high-pressure and high-temperature experiments can offer useful insight into how molecules alter under shockwave conditions.

Of the family of insensitive energetic materials, 1,3,5-triamino-2,4,6-trinitrobenzene (TATB) is the least sensitive to thermal and mechanical shock and is widely used in modern nuclear warheads.[2,5] It is so stable that it can be safely machined.[7,8] It has a relatively high density (1.94 g/cm^3). The high level of resistance to detonation is believed to be due to an extensive network of N−O and N−H bonds that produce strong intra- and intermolecular hydrogen bonding within planes of the lattice[1,9,10] and possibly π-stacked interactions.[11] It is also the reason why the solid has no observable melting point.[12] Perpendicular to the planes, much weaker van der Waals interactions manifest, giving single crystalline TATB a graphitic/layered structure[13,14] that makes it more compressible perpendicular to these planes along the *c* axis.[13] The hyperconjugated arrangement of electron donating $-NH_2$ and electron accepting $-NO_2$ groups stabilizes the molecule with respect to the aromatic benzene skeleton ring.[5] Finally, because of the aromatic nature of TATB (similar carbon skeleton to benzene), the molecule should be relatively stable because of its resonance structure.[15]

Despite the importance of this material to the U.S. Department of Energy, it has been sparsely investigated at high pressure both experimentally[1,13,16−19] and theoretically.[9,20−22] Among the varied experimental studies of TATB under extreme conditions published in the literature, visible and UV light have been shown to cause damage to TATB samples under ambient[1,17,23] and high pressures[1] (at least when using light of wavelengths shorter than 550 nm[8,17]), whereas infrared (IR) studies have not.[16] X-rays also cause damage to TATB.[13,24] Finally, in some of our recent studies on ringed hydrocarbons,[25] we have observed strong fluorescence at higher pressures in Raman studies that completely obscured spectra that we have not observed in IR studies. In our IR studies of TATB, we found no evidence of any damage of our samples due to the IR beam. Therefore, from the currently available experimental methods to study TATB samples under high pressure, IR spectroscopy would appear to be well-suited to study the molecule without damaging it and with little contaminating interference. Also, IR spectra complement Raman spectra of the same molecules, yielding a more complete spectroscopic picture of the material under extreme conditions.

It is thus in this spirit that we have continued our prior IR measurements of TATB to higher pressures. In our earlier studies,[16] we observed a decrease in the N−H stretch frequency that we attributed to an increase in hydrogen bonding with pressure along with no evidence of any phase transitions of the molecule, suggesting that the unit cell symmetry remains triclinic (space group $P\bar{1}$) with two molecules per unit cell. This

* Corresponding author. E-mail: pravica@physics.unlv.edu.
† University of Nevada Las Vegas.
‡ Carnegie Institution of Washington.

10.1021/jp903584x CCC: $40.75
Published on Web 07/16/2009

observation of the lack of any structural phase transition was supported by recent X-ray results to 10 GPa.[13]

We were thus interested in ascertaining if the observed no-phase-change behavior would continue into higher pressure regimes and also to determine if and when higher pressures would irreversibly damage the molecule to garner further insight into its stability with pressure. Hydrogen bonding appeared to increase with pressure commensurate with a decrease in N−H vibrational frequencies up to 10 GPa.[16] Does this behavior continue toward higher pressure? Does the molecule survive at higher pressures or decompose? Finally, we sought to extend our prior studies to beyond 10 GPa to further complement the Raman spectral data up to 16 GPa in the literature.[1]

Given that the sample volumes for static high-pressure experiments are typically in the 3 nL range and the sample diameters are frequently less than 100 μm, we performed the IR studies using a synchrotron light source for improved signal-to-noise and reduced acquisition times. Synchrotron light sources typically are far brighter radiation sources than blackbody sources and allow the beam to be focused to less than 10 μm (near the limits of diffraction) without significant loss of radiation.[26]

Experimental Section

Our experiments were conducted at the U2A beam station situated on the vacuum ultraviolet (VUV) ring of the National Synchrotron Light Source (NSLS) at Brookhaven National Laboratory. IR spectra were obtained within the 100−3400 cm^{-1} range. The synchrotron beam from the VUV ring is collected via a wedged diamond window, collimated, and then directed via an evacuated pipe into a Brüker IFS 66s/V Fourier transform infrared spectrometer (FTIR). The FTIR spectrometer contains three distinct microscope systems that enable measurements in the mid- and far-IR spectral regions and at variable temperature. For the mid-IR region, the beam is focused onto the sample using a nitrogen-purged IR microscope (Brüker IR Scope II), and spectra are collected either in transmission or reflection modes. For far-IR experiments, the beam is directed toward a nitrogen-purged mid-IR and far-IR microscope in which the sample chamber can be evacuated. A third microscope enables low-temperature far- and mid-IR measurements in a similarly nitrogen-purged environment and was not used in these experiments. All of the microscopes can typically focus the IR beam to a 30 μm spot that is then spatially filtered to a 20 × 20 μm^2 square except in far-IR measurements where the beam is defocused to illuminate the entire sample. (See Figure 1.) Both mid- and far-IR spectral acquisitions require sample placement into the different microscopes and thus cannot be performed simultaneously. More details regarding the experimental setup can be found in ref 27.

Our samples comprised bright-yellow TATB powder of submicrometer grain size that was supplied by Dr. Daniel Hooks of Los Alamos National Laboratory. To pressurize the samples, we used a symmetric-design diamond anvil cell (DAC)[28] that has been optimized for accommodation in the U2A's FTIR microscope system. The pressurizing diamonds were low-fluorescence type II diamonds with low IR absorption and had 300 μm diameter culets. We prepared stainless steel gaskets by preindenting them to a thicknesses of approximately 50 μm and then drilled to make ∼130 μm diameter holes via electric discharge machining. TATB powder was manually introduced onto one of the diamond flats and then gently pressed to the desired thickness (<10 μm due to the strong IR absorption by the sample). The preindented gasket thicknesses were selected to be much greater than the sample thickness to prevent the diamonds from damaging one another under load. For the far-IR experiment, the sample thickness was about 30 μm, and no pressure-transmitting medium was used. For the mid-IR experiment, the sample thickness was ∼4 μm, and roughly 1/2 of the sample region was laterally cleared of TATB to serve as a background reference. (See Figure 1.) A few ruby crystals (∼15 μm in diameter) were introduced to the mostly empty sample chamber as pressure sensors.[29] For the mid-IR experiments, the gasket hole was then filled with KBr powder, which served as the pressure-transmitting medium (KBr has negligible absorption in the mid-IR spectral region). The sample-laden DAC was manually manipulated into the focal region of the microscope objective through which the high flux polychromatic IR beam passed. The spectrometer then collected FTIR spectra downstream in transmission. The far-IR experiments required spectral acquisitions each about 15 min long. The mid-IR experiments (including the acquisition of a background spectrum) entailed roughly 10 min for each spectrum.

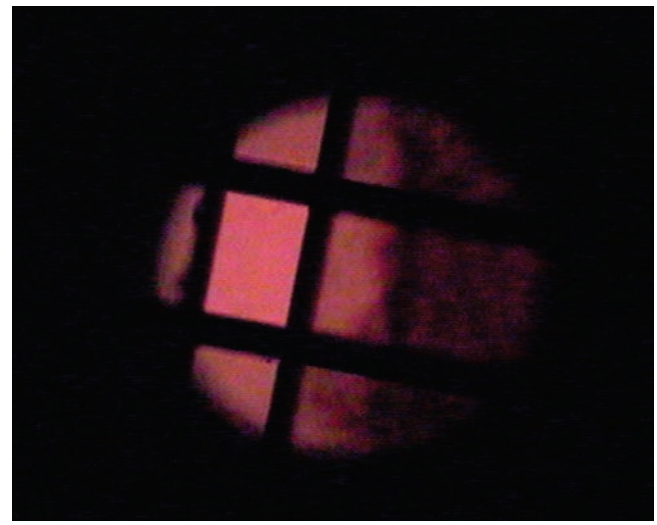

Figure 1. TATB sample near 10 GPa as seen through one diamond using the mid-IR microscope. The TATB sample is toward the right half of the sample region (less transmitted light). Spatial filtering is performed via the overlaid cross-hatching pattern seen in the Figure. In this snapshot, background is being taken from the bright full rectangle displayed.

For the mid-IR spectra, we collected background at each pressure by translating the DAC into the gasket hole region that had no TATB sample (but just KBr). The background reference spectrum was then automatically subtracted from the sample spectra. For the far-IR experiment, one background spectrum was obtained with an empty DAC in place but no gasket between the diamonds.

IR spectra were collected with each pressure increase in the sample under study (mostly in 1 to 2 GPa steps) after waiting some 20 min for the sample pressure to stabilize after pressure increase. Spectra were also recorded in both experiments as the sample pressure was reduced from the maximum value to investigate reversibility of pressure cycling. The spectral resolution for all of our measurements was roughly 4 cm^{-1}.

Results

Far-Infrared Data. We performed experiments on TATB in the far-IR range up to ∼30 GPa. Figure 2 displays some of our data in the far-IR (100−700 cm^{-1} range) region. Partially because of the large network of intra- and intermolecular

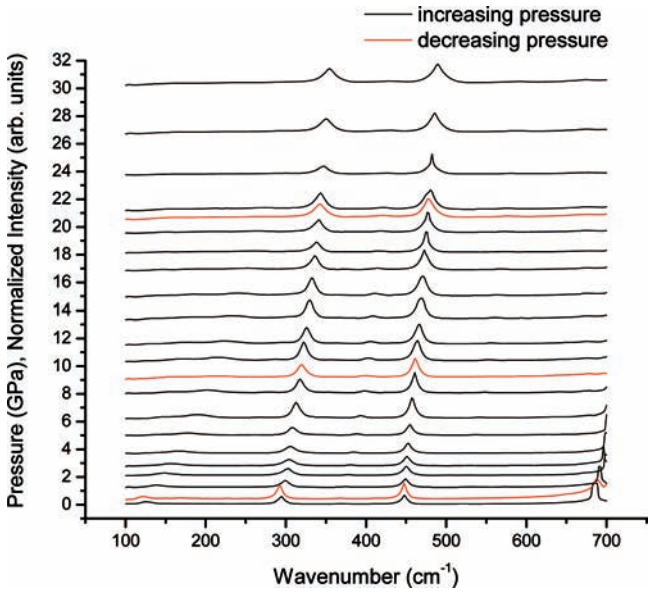

Figure 2. Far-infrared spectra of TATB with pressure. Spectral baselines are vertically displaced by the approximate pressure at which each of the spectra was acquired. Spectra printed in red dashes were taken as the sample pressure was reduced from its maximum value (decompression sequence).

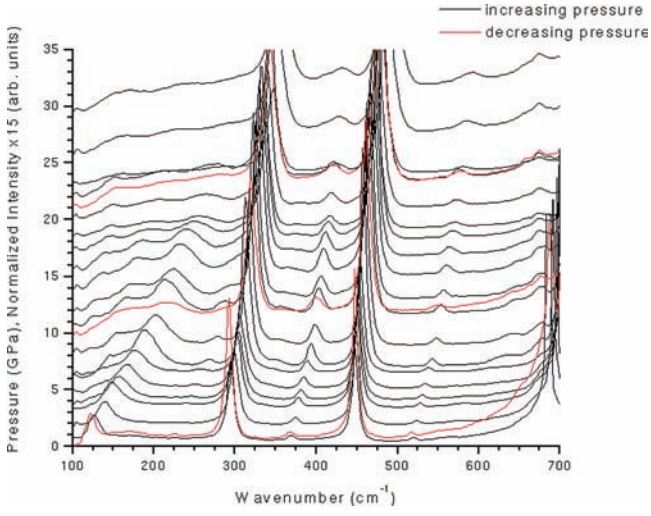

Figure 3. Amplified spectral plots from Figure 2 showing some of the weaker peaks.

hydrogen bonding, there is extensive mixing between the NO_2 and NH_2 modes,[1] and thus Vergoten[30] predicts only six pure modes under ambient conditions and neglects intermolecular hydrogen bonding,[1] of which only four are IR-active.[30] In the far-IR region we studied, no pure modes are expected to be seen. Figure 3 is an amplified version of Figure 2 to show some of the weaker peaks not readily seen there. Observed peak positions agree well at ambient pressure with the experimental results of Figure 3 of ref 30. The low frequency line near 120 cm^{-1} (seen most easily in Figure 3) has the most dramatic frequency shift with pressure up to about 20 GPa and is unassigned.[30] The major line beginning near 290 cm^{-1} at ambient pressure is of E' symmetry[21] and is assigned as a ring twist mode.[21] The other major line near 448 cm^{-1} likely represents the first overtone of the NH_2 torsion group[31] or NO_2 rocking of E' symmetry.[32] The minor line beginning near 520 cm^{-1} is a combination of the CNH_2 torsion and NO_2 bend-out-of-plane (BOP) vibrations.[30] The minor line commencing at 365 cm^{-1} is assigned as a ring deformation of E' symmetry.[21] In

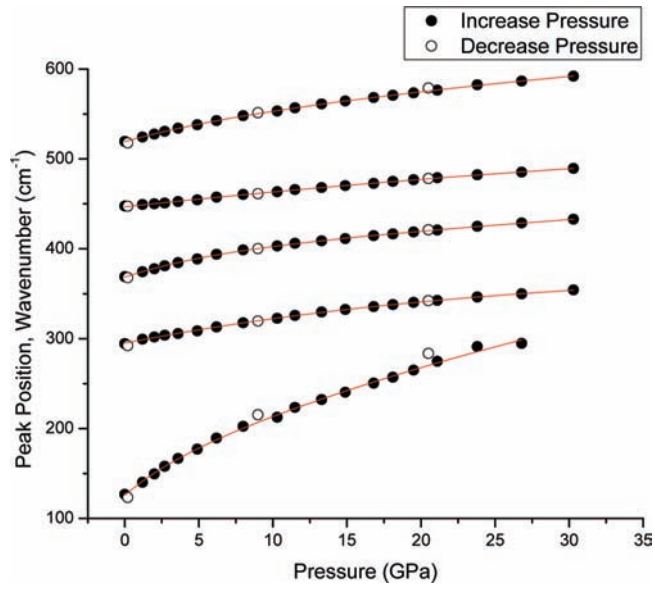

Figure 4. Selected far-IR peak positions as a function of pressure in both compression (●) and decompression (○).

examining these lines, one should bear in mind that there are some controversies associated with the modal assignments.[1] Nevertheless, all observed lines seem to shift toward higher frequencies, as expected. As seen in our earlier results,[16] we find little evidence of a phase transition up to ~30 GPa. Interestingly, the spectral line near 480 cm^{-1} in the curve at 26 GPa narrows and then broadens with higher pressure. We are uncertain as to the reason for this behavior. The opposite behavior was observed by Satija in the ν(N−O) vibration near 1170 cm^{-1} using Raman spectroscopy.[1] There is a very small peak that begins to form around 390 cm^{-1} around 26 GPa and remains at higher pressures. This could signal the beginning of a phase transition; however, because so many of the modes are mixed and these modes will alter both in line width and frequency with pressure, it is more likely (given the absence of further new peaks for such a complex molecule as TATB) that the observed new line is in fact a mode that has translated sufficiently with pressure relative to other modes in frequency to be suddenly distinguishable from the modes it was mixing with at lower pressures.

Spectra were also recorded during sample decompression in the far-IR experiment and, at the various pressures, do not appear significantly different from spectra recorded during compression. This evidence supports the view that TATB remains stable at the highest pressure studied and that the sample did not appear to decompose. Figure 4 showcases the progression of five observed far-IR line frequencies from Figures 2 and 3 with pressure. All spectral frequencies were determined by fitting peaks with Lorentzian profiles using Origin.

Mid-Infrared Data. Our mid-IR experiment ranged up to ~40 GPa. The sample thickness was ~4 μm with the remainder of material inside the sample chamber being KBr powder. The sample was typically pressurized in 1 to 2 GPa steps. Spectral patterns were acquired in the 600−4000 cm^{-1} range and are displayed in Figure 5 with the 1900−3000 cm^{-1} region of diamond absorption excised. Because of the strong intraplanar and intermolecular hydrogen bonding interactions, most of the 66 normal modes of vibration[33] mix with one another so that only about six "pure" modes are observed,[30] of which only four of these are IR modes (BOP NH_2 around 1028 cm^{-1}, bend-in-plane (BIP) NH_2 around 1219 cm^{-1}, and the NH_2 symmetric

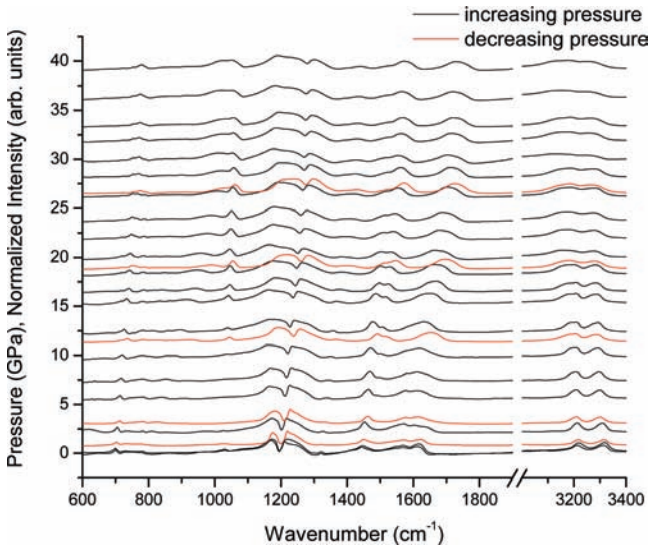

Figure 5. Midinfrared spectra of TATB at selected pressures to ~40 GPa. Baselines of the spectra are displaced vertically by the approximate pressure at which the spectra were acquired.

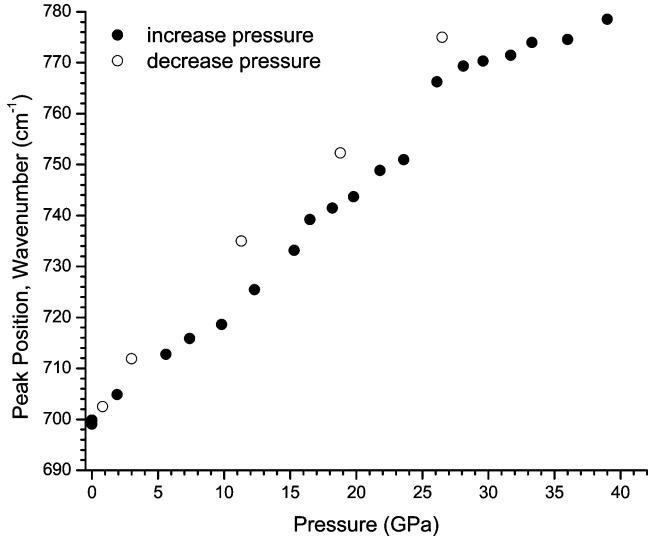

Figure 6. Peak position of a peak beginning near 700 cm^{-1} as a function of pressure in both compression and decompression. The peak is likely associated with aromatic ring and out-of-plane NH_2 vibrations.[33] The discrepancy between compression and decompression points is related to hysteresis during pressure cycling.

(υ_s) and antisymmetric (υ_a) stretches, respectively, beginning at ~3220 and ~3320 cm^{-1}, all at ambient pressure[30,31]). We have excluded the 1900−3000 cm^{-1} region in Figure 5 because it contains spectra from the diamond that confuse the interpretation of the sample data.[34] Many of the lines appear smeared/mixed, which makes interpretation difficult. No major changes are seen in the spectra as a function of pressure.

We present the evolution of frequencies of selected peaks with pressure in Figures 6−8. Of particular interest and focus in this article are the two lines beginning at ~3220 and ~3320 cm^{-1} at ambient pressure that represent the NH_2 symmetric (υ_s) and antisymmetric (υ_a) stretches, respectively,[30,31] represented in Figure 8. We have included our error bars that were determined by Origin in the *y* axis (peak position) and estimates of the errors incurred in our pressure measurements along the *x* axis.

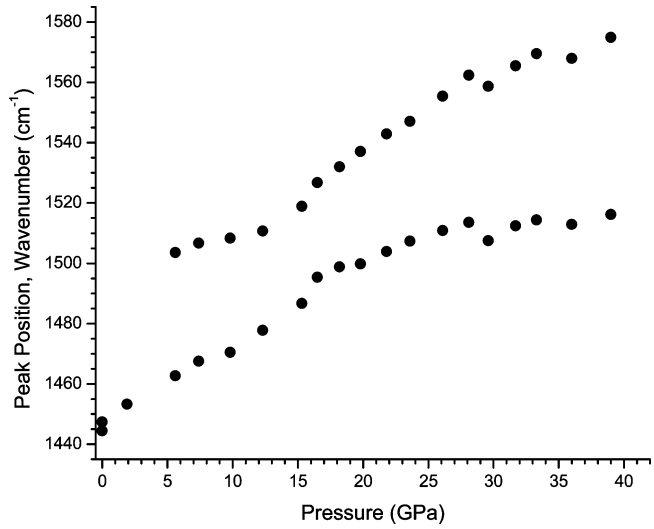

Figure 7. Peak positions of two discernible peaks beginning near 1440 and 1500 cm^{-1}, respectively, as a function of pressure. The series of points beginning near 1445 cm^{-1} is likely due to a combination of ring stretching and NH_2 rocking modes and E' symmetry.[21] The second series of points commencing around 5 GPa and 1505 cm^{-1} is unassigned.

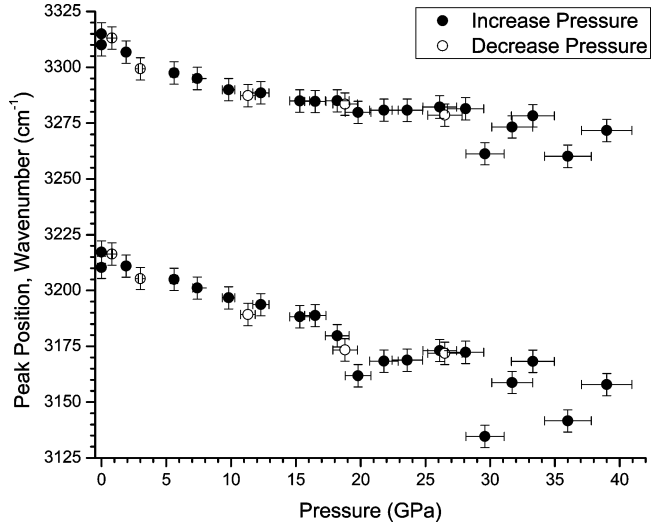

Figure 8. NH_2 symmetric stretch (bottom) and NH_2 antisymmetric stretch (top) frequencies as a function of pressure. Error bars associated with the peak fits are included.

Discussion

For both sets of experiments, the color of TATB changed from yellow → green → red → deep purple → almost black upon compression. Upon decompression of the samples, the original ambient yellow coloring of the sample returned. Examining Figures 2 and 5, we find little compelling evidence of any significant phase transitions in the examined pressure range, which agrees with earlier studies up to 16 GPa.[1,13,16] Most of the spectral lines steadily increase in frequency with pressure, as expected, except for the NH_2 vibrations near 3220 and 3320 cm^{-1}, which steadily decrease with pressure. Indeed, these two vibrations appear at 3440 and 3360 cm^{-1} in aniline and at 3470 and 3350 cm^{-1} in *para*-nitroanaline, which are higher than in TATB, lending credence to the important role of intra- and intermolecular hydrogen bonding in TATB as well as the resonance behavior of the amino group.[32] Therefore, with the application of pressure, we increase hydrogen bonding interactions as the material under study is compressed, causing a

reduction in intermolecular distances. Increasing hydrogen bonding with pressure reduces electron density in the N−H bonds, which would result in a diminished vibrational frequency. We expect similar behavior to be seen with the NO_2 vibrational modes, which was seen in ref 1. In that study, Satija et al. suggest that this frequency decrease is due to the extensive mixing of NO_2 and NH_2 vibrational modes because intermolecular hydrogen bonds strengthen with pressure as the intraplanar, intermolecular distances decrease. Inspection of Figure 5 unambiguously demonstrates that the frequencies of the N−H modes generally decrease with increasing pressure with the exception of a dip in the NH_2 symmetric stretch mode near 20 GPa and more complicated behavior in both NH_2 υ_s and υ_a vibrations around 30 GPa. Given that some NO_2 frequencies decrease as well where other molecular frequencies increase, it should be clear that the decrease in NO_2 and NH_2 frequencies are strongly coupled and that by changing pressure, molecular density is increased, which results in mostly increased intermolecular interactions. Of the possible interactions, hydrogen bonding would be the strongest. It should be noted that the detonation pressure of TATB is roughly 30 GPa,[5,9] so we are within the typical pressure of the detonation front but far below the pressure (estimated at 120 GPa[9]) for metallization. On top of this, more careful examination of Figure 5 reveals that broadening of the NH_2 stretches becomes very significant above 20 GPa, which creates difficulty in the interpretation of spectral peaks but which is also yet another possible indicator of increased hydrogen bonding with pressure. Stevens et al. suggest an interplanar dimerization between TATB layers as pressure is increased above 8 GPa, except that their observed cusp in the equation of state is within the experimental error bars.[13] Although we have observed dimerization and polymerization of benzene (a structurally related molecule)[35] and cyclooctatetraene[25] with pressure in similar pressure ranges above 10 GPa, there are no immediately obvious signs of $\pi-\pi$ dimerization in our results here.

Conclusions

We have continued our study of an important secondary high explosive, TATB, with pressure using IR spectroscopy, quadrupling the investigated pressure range. We have further confirmed the general trend that the NH_2 vibrational symmetric and antisymmetric modes decrease with pressure, which we attribute to increasing intermolecular hydrogen bonding (because of decreased intermolecular distances and interplanar spacing) that weakens these molecular bonds via partial electron transfer. We have found little evidence of any significant phase transitions or irreversible molecular decomposition up to the highest pressures studied. This lends credence to the incredible stability of this insensitive explosive with pressure and the importance of hydrogen bonding in determining TATB's behavior under pressure. Further work will aim to interrogate molecular alterations above 40 GPa.

Acknowledgment. We gratefully acknowledge support from the U.S. Army RDECOM ACQ CTR contract W9011NF-05-1-0266, the Nevada/NASA space grant, and the DOE DE-FC88-06NA27684 Cooperative Agreement with UNLV. Use of the National Synchrotron Light Source is supported by the DOE Office of Science, Office of Basic Energy Sciences under contract no. DE-AC02-98CH10886. The U2A beamline is supported by COMPRES, the Consortium for Materials Properties Research in Earth Sciences, under NSF Cooperative Agreement grant no. EAR01-35554 and the U.S. DOE (CDAC, contract no. DEFC03-03N00144).

References and Notes

(1) Satija, S. K.; Swanson, B.; Eckert, J.; Goldstone, J. A. *J. Phys. Chem.* **1991**, *95*, 10103–10109.
(2) Cooper, P. W. *Explosives Engineering*; Wiley-VCH: New York, 1996.
(3) Dlott, D. D.; Fayer, M. D. *J. Chem. Phys.* **1990**, *92*, 3798–3812.
(4) Kunz, A. B.; Kuklja, M. M.; Botcher, T. R.; Russell, T. P. *Thermochim. Acta* **2002**, *384*, 279–284.
(5) Badgujar, D. M.; Talawar, M. B.; Asthana, S. N.; Mahulikar, P. P. *J. Hazard. Mater.* **2008**, *151*, 289–305.
(6) Tarver, C. *Shock Compression Condens. Matter* **2001**, *CP620*, 42–49.
(7) Son, S. F.; Assay, B. W.; Henson, B. F.; Sander, R. K.; Ali, A. N.; Zielinski, D. S.; Phillips, D. S.; Schwarz, R. B.; Skidmore, C. B. *J. Phys. Chem.* **1999**, *103*, 5434–5440.
(8) Dobratz, B. M. *The Insensitive High Explosive Triaminotrinitrobenzene (TATB): Development and Characterization- 1888 to 1994*; Los Alamos Technical Report LA-13014-H; Los Alamos National Laboratory: Los Alamos, NM, 1995.
(9) Wu, C. J.; Yang, L. H.; Fried, L. E.; Quenneville, J.; Martinez, T. J. *Phys. Rev. B* **2003**, *67*, 235101.
(10) Rogers, J. W., Jr.; Peebles, H. C.; Rye, R. R.; Houston, J. E.; Binkley, J. S. *J. Chem. Phys.* **1984**, *80*, 4513–4520.
(11) Zhang, C.; Wang, X.; Huang, H. *J. Am. Chem. Soc.* **2008**, *130*, 8359–8365.
(12) Cady, H. H.; Larson, A. C. *Acta Crystallogr.* **1965**, *18*, 485–496.
(13) Stevens, L. L.; Velisavljevic, N.; Hooks, D. E.; Dattelbaum, D. M. *Propellants, Explos., Pyrotech.* **2008**, *33*, 286–295.
(14) Zhang, C. *J. Phys. Chem. B* **2007**, *111*, 14295–14298.
(15) Wade, L. G., Jr. *Organic Chemistry*, 5th ed.; Prentice Hall: Upper Saddle River, NJ, 2003; p 69.
(16) Pravica, M.; Yulga, B.; Liu, Z.; Tschauner, O. *Phys. Rev. B.* **2007**, *76*, 064102.
(17) Holy, J. *J. Phys. Chem. B* **2008**, *112*, 7489–7498.
(18) Grebenkin, K. F.; Zherebtsov, A. L. *Combus., Explos., Shock Waves* **2000**, *36*, 246–261.
(19) Olinger, B.; Cady, H. In *Proceedings/Sixth Symposium (International) on Detonation*; Office of Naval Research, Department of the Navy: Arlington, VA, 1976; p 224.
(20) Zhang, C.; Shu, Y.; Zhao, X.; Wang, X. *Sci. Technol. Energ. Mater.* **2005**, *66*, 261–265.
(21) Liu, H.; Zhao, J.; Ji, G.; Wei, D.; Gong, Z. *Phys. Lett. A* **2006**, *358*, 63–69.
(22) Byrd, E. F. C.; Rice, B. M. *J. Phys. Chem. C* **2007**, *111*, 2787–2796.
(23) Williams, D. L.; Timmons, J. C.; Woodyard, J. D.; Rainwater, K. A.; Lightfoot, J. M.; Richardson, B. R.; Burgess, C. E.; Heh, J. L. *J. Phys. Chem. A* **2003**, *107*, 949–9494.
(24) Giefers, H.; Pravica, M. *J. Phys. Chem. A* **2008**, *112*, 3352–3359.
(25) Tkachev, S.; Pravica, M.; Kim, E.; Romano, E.; Weck, P. F. *J. Phys. Chem. A* **2008**, *112*, 11501–11507.
(26) See, for example: http://www.esrf.eu/UsersAndScience/Experiments/Imaging/ID21/SrFtir/FtirIntro.
(27) Liu, Z.; Hu, J.; Yang, H.; Mao, H. K.; Hemley, R. J. *J. Phys.: Condens. Matter* **2002**, *14*, 10641–10646.
(28) Dunstan, D. J.; Spain, I. L. *J. Phys. E: Sci. Instrum* **1989**, *22*, 913–933.
(29) Piermarini, G. J.; Block, S.; Barnett, J. D.; Forman, R. A. *J. Appl. Phys.* **1975**, *46*, 2774–2780.
(30) Vergoten, G.; Fleury, G.; Blain, M.; Odiot, S. *J. Raman Spectrosc.* **1985**, *16*, 143–148.
(31) Towns, T. G. *Spectrochim. Acta* **1983**, *39A*, 801–804.
(32) Deopura, B. L.; Gupta, V. D. *J. Chem. Phys.* **1970**, *54*, 4013–4019.
(33) Huang, Z.; Chen, B.; Gao, G. *J. Mol. Struct.* **2005**, *752*, 87–92.
(34) Zaitsev, A. *Optical Properties of a Diamond*; Springer: New York, 2001.
(35) Pravica, M.; Grubor-Urosevic, O.; Hu, M.; Chow, P.; Liermann, P. *J. Phys. Chem. B* **2007**, *111*, 11635–11637.

JP903584X